

# Experimental and theoretical approach for the clustering of globally coupled density oscillators based on phase response

Masanobu Horie, Tatsunari Sakurai, and Hiroyuki Kitahata\*

*Department of Physics, Graduate School of Science, Chiba University, Chiba 263-8522, Japan*

(Received 15 October 2015; published 20 January 2016)

We investigated the phase-response curve of a coupled system of density oscillators with an analytical approach. The behaviors of two-, three-, and four-coupled systems seen in the experiments were reproduced by the model considering the phase-response curve. Especially in a four-coupled system, the clustering state and its incidence rate as functions of the coupling strength are well reproduced with this approach. Moreover, we confirmed that the shape of the phase-response curve we obtained analytically was close to that observed in the experiment where a perturbation is added to a single-density oscillator. We expect that this approach to obtaining the phase-response curve is general in the sense that it could be applied to coupled systems of other oscillators such as electrical-circuit oscillators, metronomes, and so on.

DOI: [10.1103/PhysRevE.93.012212](https://doi.org/10.1103/PhysRevE.93.012212)

## I. INTRODUCTION

Many phenomena seen in biology, chemistry, physics, and other fields can be discussed by being simplified as coupled nonlinear oscillators [1–11]. It has been reported that such coupled nonlinear oscillators can exhibit various kinds of behaviors, such as perfect synchronization,  $N$ -phase modes, chaos, and clustering [1]. Among them, the clustering of coupled nonlinear oscillators has been attracting increasing interest. Generally, nonlinear oscillators are described by sets of nonlinear differential equations. Thus, it is difficult to understand how clustering occurs directly from the form of the differential equations. To attain an analytical understanding of the mechanism of clustering, numerous studies have been conducted mainly with a theoretical approach. For example, Kori *et al.* investigated the clustering of coupled electrochemical oscillators. In their study, they analyzed the clustering phenomena under the assumption that the system is near the bifurcation point [12].

Density oscillators have been investigated as a good experimental system for a sustained nonlinear oscillator, which was first introduced by Martin [13]. When a higher-density fluid is put in a smaller vessel with a bore at its bottom, and the smaller vessel is settled in a lower-density fluid in a larger vessel, upward flow of the lower-density fluid and downward flow of the higher-density fluid recurs; this is called density oscillation. When two density oscillators are coupled, i.e., two smaller vessels are settled in one larger vessel, antiphase synchronization occurs. It is also known that an  $N$ -coupled system can show an  $N$ -phase mode or clustering in certain situations [3,14,15]. In the density oscillation, switching between upward and downward flow is important, and it is difficult for us to adopt the theory near the bifurcation points. In previous studies, various mathematical models for density oscillators have been proposed. Some of them use a form of Rayleigh equation [14–16], whereas others investigated the mechanism regarding the pressure change based on hydrodynamics [17–19]. González *et al.* measured the phase responses experimentally and discussed

the phase-response curve [20], but they did not investigate the coupled systems.

In the present article, we consider coupled sustained nonlinear oscillators represented by density oscillators. We employ a phase description of the density oscillators to try to understand the clustering of the coupled system. First, we introduce the experimental results for the coupled density oscillators and show the existence of the clustering mode for four-coupled oscillators. Then, we construct the model equation for the density oscillator based on the phase description. To confirm the validity of the phase description, we compared the analytical results with the experimental ones for two-, three-, and four-coupled density oscillators. We also measured the phase-response curve experimentally and compared our measurements with the analytical results. The present study will help our understanding of coupled nonlinear sustained oscillators.

## II. EXPERIMENT: SYNCHRONIZATION OF A COUPLED SYSTEM

First, we observed synchronization of density oscillators to investigate the characteristics of a coupled system of density oscillators. The experimental setup is shown in Fig. 1.

A large vessel containing a low-density fluid was prepared, and small vessels containing a high-density fluid were put inside it. These inner vessels had nearly identical bores of diameters  $\sim 1$  mm at their bottoms. We used fresh water (density  $\rho = 1.00$  g/ml) as the low-density fluid and saline water (density  $\rho' = 1.14$  g/ml) as the high-density fluid. The surface area of the inner vessel,  $S'$ , was fixed at  $1200$  mm<sup>2</sup>, and we observed the behavior of the system as the surface area of the outer vessel,  $S$ , was changed from  $1300$  to  $10\,700$  mm<sup>2</sup>. When  $S = 2000$  mm<sup>2</sup>, the intrinsic period of one oscillator without coupling was  $25 \pm 1$  s. Additionally, the coupling strength is known as an increasing function of  $S'/S$ . Thus we conducted experiments under various coupling strengths.

To compare the behavior of the experimental system with that of the phase oscillator model, we need to extract phases of oscillators from the experimental results. To do so, we first measured the brightness at points just below the bores of the

\*kitahata@chiba-u.jp

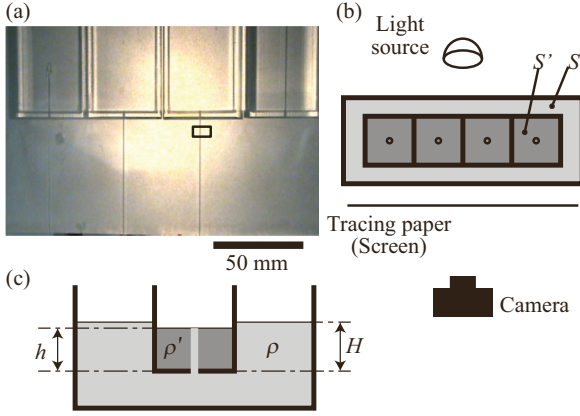


FIG. 1. Experimental system: (a) Snapshot of side view. (b) Schematic illustration of the top view.  $S$  and  $S'$  denote surface areas of the outer and inner vessel, respectively. (c) Schematic illustration of the side view.  $H$  and  $h$  denote the water levels from the height of the bore outside and inside the vessel, respectively.

small vessels as a function of time, as shown in Fig. 2. The time resolution of this measurement was 0.1 s.

In this time course, regions of higher and lower brightness correspond to upflow and downflow, respectively. Therefore, we defined each time when flow changes from downward to upward as corresponding to the origin of the phase; phases of other states are defined via linear interpolation, with the phase difference  $\Delta\phi_i$  of the  $i$ th oscillator from the  $N$ th oscillator being defined by  $\Delta\phi_i = \phi_i - \phi_N$ . Of course, the phases defined as above are not exact especially on a short timescale, i.e., in one or two periods, but we are interested in the phenomena on a long timescale and so the phase description works in such a case. In fact, synchronization and clustering usually last more than ten periods. Hence, inaccuracy from data processing can be neglected.

Experimental results for two and three coupled oscillators are shown in Fig. 3. In a two-coupled system, antiphase synchronization was observed, and a three-phase mode with a phase differences of  $2\pi/3$  appeared in a three-coupled system.

Results for a four-coupled system are shown in Fig. 4. Generally, the clustering state was more likely to appear for smaller  $S$ , i.e., stronger coupling. To evaluate this tendency quantitatively, we defined criteria to determine the state of the system for an arbitrary combination of phase differences  $\Delta\phi_{i,j} = \phi_i - \phi_j$ , ( $i, j = 1, \dots, 4$  and  $i \neq j$ ) as follows:

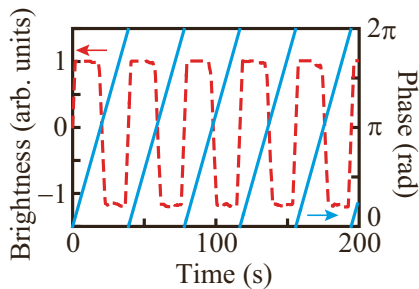


FIG. 2. Time series of the brightness (dashed curve) and phase (solid curve), where the brightness was measured in the box in the snapshot shown in Fig. 1(a).

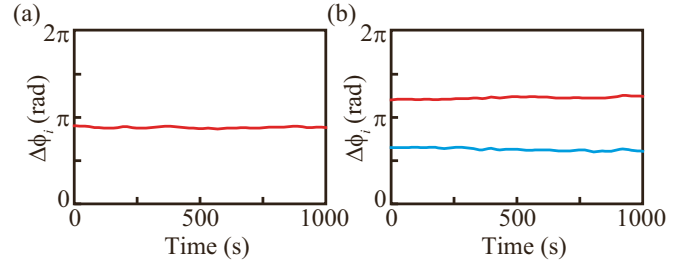


FIG. 3. Time evolution of the phase difference in (a) a two-coupled system and (b) a three-coupled system observed in the experiments. In both cases,  $S = 4000 \text{ mm}^2$  and  $S' = 1200 \text{ mm}^2$ .

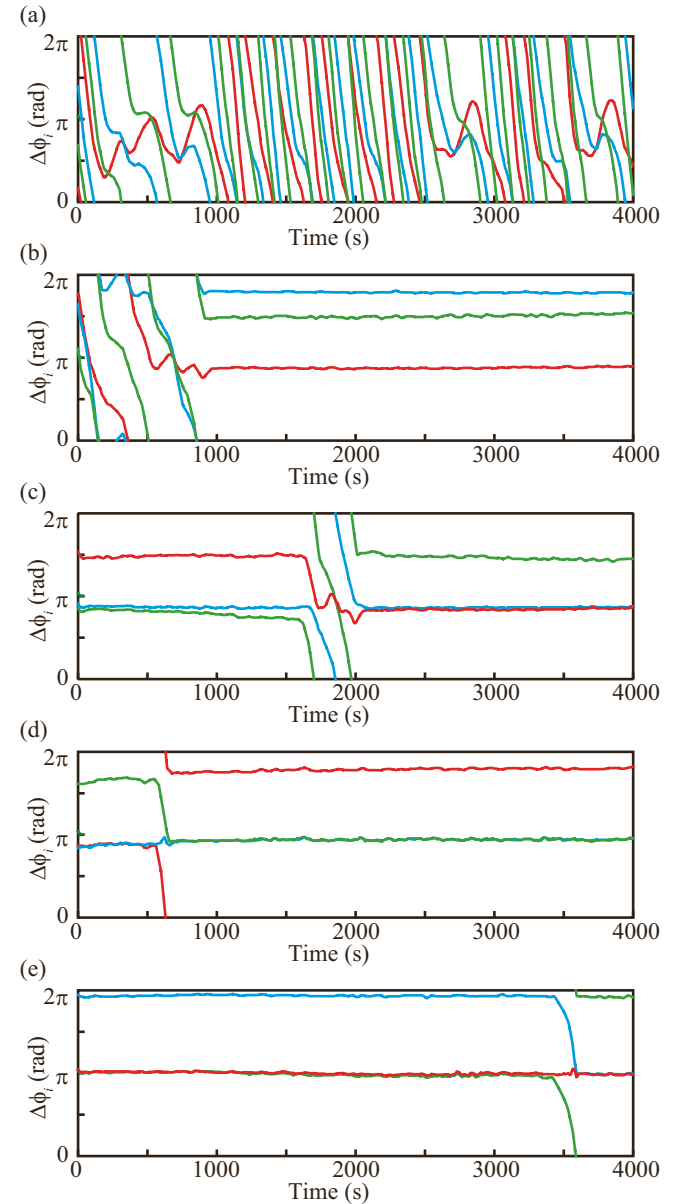


FIG. 4. Time evolution of the phase difference in a four-coupled system observed in experiments. We changed the coupling strength, which is a decreasing function of  $S$ . (a)  $S = 10700 \text{ mm}^2$ , (b)  $S = 6700 \text{ mm}^2$ , (c)  $S = 4000 \text{ mm}^2$ , (d)  $S = 2000 \text{ mm}^2$ , and (e)  $S = 1300 \text{ mm}^2$ .  $S' = 1200 \text{ mm}^2$  for all cases.

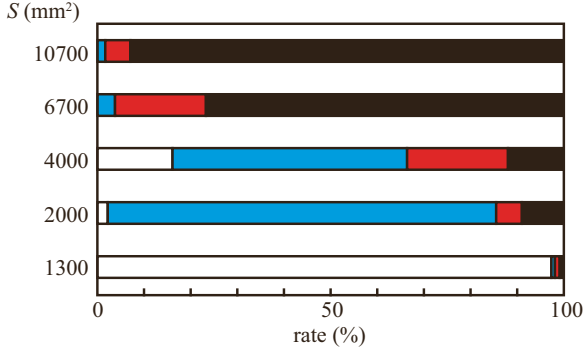


FIG. 5. Proportion of the time duration for each state in a four-coupled system with various coupling strengths. White bars denote 2-2 cluster states, light blue (light gray) 2-1-1 cluster states, red (dark gray) phase locked states, and black asynchronous states. Total experimental times are 11 225, 24 921, 44 073, 38 172, and 15 986 s for  $S = 10700, 6700, 4000, 2000,$  and  $1300 \text{ mm}^2$ , respectively.

1. Phase locking: Time change of the phase difference is smaller than a threshold, i.e.,  $|\Delta\phi_{i,j}(t + \Delta t) - \Delta\phi_{i,j}(t)|/\Delta t < 2\pi\epsilon_{\text{lock}}/\Delta t$ .

2. Clustering: The phase is locked, and the phase difference is smaller than a threshold, i.e.,  $\Delta\phi_{i,j}(t) < 2\pi\epsilon_{\text{cluster}}$ .

In this analysis,  $\epsilon_{\text{lock}} = 0.0005$  and  $\epsilon_{\text{cluster}} = 0.05$ . Based on these criteria, we separated the system into four states as follows:

1. Two-cluster state: Two oscillators are in phase (clustering), and the other two oscillators are also in phase (clustering). Two sets of the two oscillators keep the same phase difference (phase locking). This state is also called the 2-2 cluster state.

2. Three-cluster state: Two oscillators are in phase (clustering), and the other two oscillators are at phases that are different from each other (phase locking). This state is also called 2-1-1 cluster state.

3. Phase-locked state: The phase is locked without clustering. Strictly, the clustering state is also a phase-locked state. However, for convenience, we isolate the clustering state from the phase-locked state in this article.

4. Asynchronous state: This is the state of a system that is not in one of the above states.

In Fig. 5, the proportion of time in which the system is in each state is seen to depend on the coupling strength. In each condition, from two to four experiments were performed.

As we can see from Fig. 5, the two-cluster state (2-2 cluster state) appeared most frequently in the system with the strongest coupling. As coupling strength decreases, the three-cluster state (2-1-1 cluster state), the phase-locked state, and asynchronous state appeared in this order. This means that, with sufficient strength of coupling, the two-cluster state (2-2 cluster state) would be most likely to appear. Of course, this result depends on the threshold values, but over a broad range of threshold values, the same trend was observed.

### III. MATHEMATICAL MODEL

In this section, we discuss the mathematical model that reflects the features of the experimental system. First, we consider a single oscillator with a perturbation used to obtain

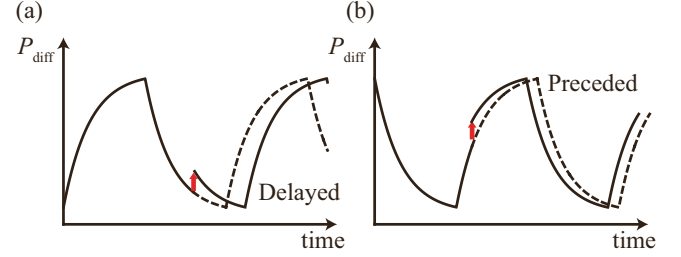


FIG. 6. Schematic illustration of the phase response in a density oscillator. (a) In the case of upflow. (b) In the case of downflow. Whether the phase is preceded or delayed depends on the state in which the perturbation is added.

a phase response, and then a coupled system is taken into account.

One possible cause of synchronization in coupled density oscillators is the change in the water level in the outer vessel. Therefore, we regard the change in the water level in the outer vessel as the perturbation. Let  $P$  and  $P'$  denote the water pressure at the bottom of a bore and at the top of a bore, respectively. That is,  $P = \rho g H$  and  $P' = \rho' g h$ , where  $\rho$  and  $\rho'$  are the densities of the low-density and the high-density fluids, respectively, and  $g$  is the gravity acceleration.  $H$  and  $h$  are the water levels in the outer and inner vessels, respectively.  $h = H = 0$  corresponds to the height of the bore. Additionally, pressure difference is defined as  $P_{\text{diff}} = P - P'$ . We hypothesize that switching from upflow to downflow and from downflow to upflow occurs at each constant value of  $P_{\text{diff}}$ .

When downflow occurs,  $P_{\text{diff}}$  increases owing to the increase in water level in the outer vessel and decrease in water level in the inner vessel. If some water is poured into the outer vessel during downflow,  $P_{\text{diff}}$  suffers additional sudden increase. This increase in  $P_{\text{diff}}$  leads to flow-switching earlier, which means the phase is preceded. In contrast, if the system is perturbed in the same way during upflow, the phase is delayed (Fig. 6).

Let us describe the idea more precisely. The time evolution of water level in each vessel can be expressed by using a combination of exponential functions [16]. In addition, we impose conservation of flow,  $S\dot{H} = -S'\dot{h}$ , and we get the following relation between the water level and the phase:

$$h(\phi) = \begin{cases} ae^{-\alpha\phi} + b, & (0 \leq \phi < \pi) \\ -ae^{-\alpha(\phi-\pi)} + b', & (\pi \leq \phi < 2\pi) \end{cases}, \quad (1)$$

$$H(\phi) = \begin{cases} -\frac{S}{S'}ae^{-\alpha\phi} + B, & (0 \leq \phi < \pi) \\ \frac{S}{S'}ae^{-\alpha(\phi-\pi)} + B', & (\pi \leq \phi < 2\pi) \end{cases}, \quad (2)$$

where  $a, b, b', B,$  and  $B'$  are fitting parameters set so that they satisfy the continuity conditions  $h(0) = h(2\pi), \lim_{\phi \rightarrow \pi+0} h(\phi) = \lim_{\phi \rightarrow \pi-0} h(\phi), H(0) = H(2\pi),$  and  $\lim_{\phi \rightarrow \pi+0} H(\phi) = \lim_{\phi \rightarrow \pi-0} H(\phi).$   $\alpha$  is also a parameter, with  $2\pi/\alpha$  denoting the characteristic time. In this model, we assume the switching of flow occurs at  $\phi = 0$  and  $\pi$ .

Using Eqs. (1) and (2), we can obtain the relationship between  $P_{\text{diff}}$  and  $\phi$  from  $P_{\text{diff}} = \rho g H - \rho' g h$  as

$$P_{\text{diff}}(\phi) = \begin{cases} -\left(\rho \frac{S}{S'} + \rho'\right) g a e^{-\alpha\phi} + D, & (0 \leq \phi < \pi) \\ \left(\rho \frac{S}{S'} + \rho'\right) g a e^{-\alpha(\phi-\pi)} + D'. & (\pi \leq \phi < 2\pi) \end{cases}. \quad (3)$$

Here,  $D$  and  $D'$  are also parameters decided by the continuity conditions. Based on this expression of pressure difference, we can discuss the phase response. We assume that pouring some water into the outer vessel corresponds to the extra addition to the pressure  $P_{\text{diff}}$  by a small amount  $\Delta P_{\text{ext}}$ . Here, we consider the pressure increase within the first order of the phase shift  $\Delta\phi_{\text{ext}}$ :

$$\Delta P_{\text{ext}} = \frac{dP_{\text{diff}}}{d\phi} \Delta\phi_{\text{ext}}. \quad (4)$$

Thus, we find the following time-evolutional equation of the phase shift unless  $dP_{\text{diff}}/d\phi$  is zero:

$$\frac{d\phi_{\text{ext}}}{dt} = \left(\frac{dP_{\text{diff}}}{d\phi}\right)^{-1} \frac{dP_{\text{ext}}}{dt}. \quad (5)$$

Here,  $d\phi_{\text{ext}}/dt$  stands for the phase shift resulting from the perturbation. Thus, the time evolution of the phase of a single density oscillator can be expressed as

$$\frac{d\phi}{dt} = \omega + \frac{d\phi_{\text{ext}}}{dt} = \omega + \left(\frac{dP_{\text{diff}}}{d\phi}\right)^{-1} \frac{dP_{\text{ext}}}{dt}. \quad (6)$$

It is remarkable that the description in Eq. (6) resembles the phase oscillator model [1,21]. We can regard the factor  $(dP_{\text{diff}}/d\phi)^{-1}$  as phase response and the factor  $dP_{\text{ext}}/dt$  as a perturbation. Therefore, if we can devise a relation between the phase and an essential physical quantity that responds to a perturbation, we can obtain the phase response according to Eq. (6). The analytical form of the phase response of a density oscillator is

$$\zeta(\phi) = \left(\frac{dP_{\text{diff}}}{d\phi}\right)^{-1} = \left[-g \left(\frac{S}{S'}\rho + \rho'\right) \frac{dh}{d\phi}\right]^{-1}. \quad (7)$$

Now, we consider a coupled system. We assume that the perturbation comes only from the pressure change resulting from the flow by the other oscillators. That is, in a coupled system, one oscillator changes the water level in the outer vessel, and this change can be regarded as a perturbation for the other oscillators.

First, we define the phase and the inner water level of the  $i$ th oscillator as  $\phi_i$  and  $h_i$ , respectively. Additionally, to simplify the problem, we assume that the parameters for each oscillator such as  $\rho'$ ,  $S'$ , and  $\omega$  are identical. In an  $N$ -coupled system, conservation of flow is expressed as

$$S\dot{H} = -\sum_k^N S'\dot{h}_k. \quad (8)$$

The pressure exerted from the outside to the inside of one oscillator is

$$P = \rho g H. \quad (9)$$

Now, the external pressure change caused by the  $i$ th oscillator,  $P_{\text{ext},i}$ , should be expressed as the difference between the outside pressure  $P$  and the outside pressure change caused by the  $i$ th oscillator. Thus,

$$\frac{dP_{\text{ext},i}}{dt} = \dot{P} - \left(-\rho g \frac{S'}{S} \dot{h}_i\right) = -\rho g \frac{S'}{S} \sum_{j \neq i} \dot{h}_j. \quad (10)$$

Here, Eqs. (8) and (9) are used. Therefore, the time evolution of the  $i$ th density oscillator in an  $N$ -coupled system can be described as

$$\frac{d\phi_i}{dt} = \omega + \left[-g \left(\frac{S}{S'}\rho + \rho'\right) \frac{dh_i}{d\phi_i}\right]^{-1} \left(-\rho g \frac{S'}{S} \sum_{j \neq i} \dot{h}_j\right). \quad (11)$$

However, this equation is not closed with respect to phases, since the factors  $\dot{h}_j$  are functions of time  $t$ . To transform this equation into a equation closed with respect to phases, we expand  $\dot{h}_j$  under the assumption that the coupling is sufficiently weak; that is, the coupling is considered to be of the order of  $\varepsilon$ . Then we can derive

$$\frac{d\phi_i}{dt} = \omega + \varepsilon \left[-g \left(\frac{S}{S'}\rho + \rho'\right) \frac{dh_i}{d\phi_i}\right]^{-1} \left(-\rho g \frac{S'}{S} \sum_{j \neq i} \dot{h}_j\right), \quad (12)$$

and

$$\dot{h}_j = \frac{dh_j}{d\phi_j} \frac{d\phi}{dt} = \frac{dh_j}{d\phi_j} [\omega + O(\varepsilon)]. \quad (13)$$

By substituting this into the Eq. (12) and neglecting the second- and higher-terms of  $\varepsilon$ , we obtain

$$\begin{aligned} \frac{d\phi_i}{dt} &= \omega + \varepsilon \left[-g \left(\frac{S}{S'}\rho + \rho'\right) \frac{dh_i}{d\phi_i}\right]^{-1} \left(-\rho g \omega \frac{S'}{S} \sum_{j \neq i} \frac{dh_j}{d\phi_j}\right) \\ &= \omega + \varepsilon \omega \frac{\rho}{\rho + \frac{S'}{S}\rho'} \left(\frac{S'}{S}\right)^2 \left(\frac{dh_i}{d\phi_i}\right)^{-1} \sum_{j \neq i} \frac{dh_j}{d\phi_j}. \end{aligned} \quad (14)$$

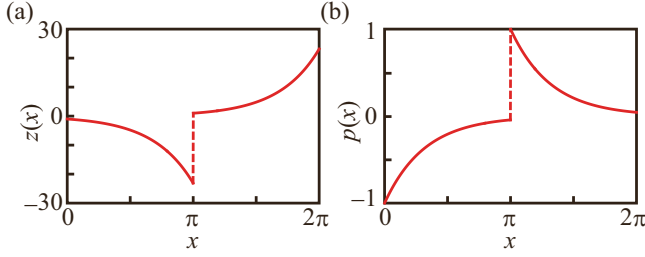
To simplify the equation, we define the strength of the coupling,  $K$ , the phase-response function,  $z(x)$ , and the equivalent external force from one oscillator,  $p(x)$ , as

$$K = \varepsilon \omega \frac{\rho}{\rho + \frac{S'}{S}\rho'} \left(\frac{S'}{S}\right)^2, \quad (15)$$

$$z(x) = \begin{cases} -e^{\alpha x}, & (0 \leq x < \pi) \\ e^{\alpha(x-\pi)}, & (\pi \leq x < 2\pi) \end{cases}, \quad (16)$$

$$p(x) = \begin{cases} -e^{-\alpha x}, & (0 \leq x < \pi) \\ e^{-\alpha(x-\pi)}. & (\pi \leq x < 2\pi) \end{cases}. \quad (17)$$

The above description shows that the coupling strength  $K$  is an increasing function of  $S'/S$ , as has been known empirically. Profiles of  $z(x)$  and  $p(x)$  are shown in Fig. 7. The signs of  $z(x)$  and  $p(x)$  are defined so that  $z(x)$  exhibits the same behavior as  $\zeta(x)$ . By using these definitions, the time evolution of the

FIG. 7. Profiles of  $z(x)$  and  $p(x)$  plotted with  $\alpha = 1.0$ .

phase can be expressed as

$$\frac{d\phi_i}{dt} = \omega + K z(\phi_i) \sum_{j \neq i} p(\phi_j). \quad (18)$$

When coupling between oscillators is weak enough for the phase change to be sufficiently small during one oscillation period, the coupling function can be averaged over the oscillation period. Through averaging, the coupling function can be written as a function depending only on a phase difference. In general, for a weakly coupled oscillator,

$$\frac{d\phi_i}{dt} = \omega + K \sum_{j \neq i} f(\phi_i, \phi_j), \quad (19)$$

can be averaged as

$$\frac{d\phi_i}{dt} = \omega + K \sum_{j \neq i} \Gamma(\phi_i - \phi_j), \quad (20)$$

where

$$\Gamma(x) = \frac{1}{2\pi} \int_0^{2\pi} d\psi f(x + \psi, \psi). \quad (21)$$

The averaged coupling function in a coupled system of density oscillators is

$$\begin{aligned} \Gamma(x) &= \frac{1}{2\pi} \int_0^{2\pi} d\psi z(x + \psi) p(\psi) \\ &= \begin{cases} -\frac{1}{\pi} [x e^{-\alpha(\pi-x)} - (\pi-x) e^{\alpha x}] & (0 \leq x < \pi) \\ \frac{1}{\pi} [(x-\pi) e^{-\alpha(2\pi-x)} - (2\pi-x) e^{\alpha(x-\pi)}] & (\pi \leq x < 2\pi) \end{cases}, \quad (22) \end{aligned}$$

which is plotted in Fig. 8(a).

#### IV. ANALYSIS AND NUMERICAL CALCULATION

By using both nonaveraged and averaged model equations obtained in the previous section, we performed a linear stability analysis and a numerical calculation. For the linear stability analysis, we define the phase difference  $\psi_i$  and a small difference from the fixed point  $\theta_i$  ( $i = 1, 2, \dots, N-1$ ) as

$$\psi_i = \phi_i - \phi_N, \quad (23)$$

$$\theta_i = \psi_i - \psi_i^* \quad (\theta_i \ll 1), \quad (24)$$

where  $N$  is the number of the oscillators in the coupled system, and  $\psi_i^*$  is the fixed point.

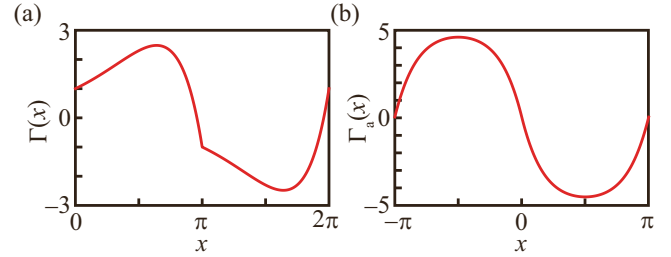


FIG. 8. (a) Profile of the averaged coupling function for a density oscillator. (b) Relation between  $\Gamma_a(x) = \Gamma(\pi+x) - \Gamma(\pi-x)$  and  $x$ . The slope of the curve is negative around  $x = 0$ , which means that the two-coupled oscillators exhibit stable antiphase synchronization. Here we set  $\alpha = 1.0$ .

For the numerical calculation, we computed the time evolution of the obtained phase model under an angular velocity  $\omega = 2\pi/25$  with  $N = 2, 3$ , and 4 oscillators by using the Euler method. For all cases, initial phase of each oscillator is determined by using a uniform pseudorandom number in  $[0, 2\pi)$  and the time step is set to be 0.001.

#### A. Two-coupled system

First, we perform a linear stability analysis for a nonaveraged coupling system. A two-coupled system with nonaveraged coupling can be expressed as

$$\frac{d\phi_1}{dt} = \omega + K z(\phi_1) p(\phi_2), \quad (25a)$$

$$\frac{d\phi_2}{dt} = \omega + K z(\phi_2) p(\phi_1). \quad (25b)$$

Then, we assume  $0 \leq \phi_2 < \pi \leq \phi_1 < 2\pi$ . By changing the indices of the oscillators, the condition  $0 \leq \phi_1 < \pi \leq \phi_2 < 2\pi$  is always satisfied. The fixed point we focus on is  $\psi_1^* = \pi$ . By making  $\theta_1$  close enough to 0, the duration satisfying  $0 \leq \phi_1, \phi_2 < \pi$ , or  $\pi \leq \phi_1, \phi_2 < 2\pi$  can be made short enough to be negligible.

The synchronous state is expressed as  $\dot{\psi}_1 = 0$ . Analyzing the stability of the synchronous state entails only the stability around the fixed point of  $\psi_1$ . The equation to be analyzed is

$$\frac{d\psi_1}{dt} = K z(\phi_1) p(\phi_2) - K z(\phi_2) p(\phi_1) \quad (26)$$

$$= -K (e^{\alpha(\psi_1-\pi)} - e^{-\alpha(\psi_1-\pi)}). \quad (27)$$

In this equation, we can see that  $\psi_1 = \pi$  is a fixed point. To analyze the stability, we consider

$$\frac{d\theta_1}{dt} \simeq -\alpha K (e^{\alpha\theta_1} + e^{-\alpha\theta_1})|_{\theta_1=0} \theta_1 = -2\alpha K \theta_1. \quad (28)$$

Since  $-2\alpha K < 0$ , antiphase synchronization is stable in the nonaveraged coupled system.

In the averaged coupling system, we obtain

$$\frac{d\theta_1}{dt} = K \Gamma_a(\theta_1), \quad (29)$$



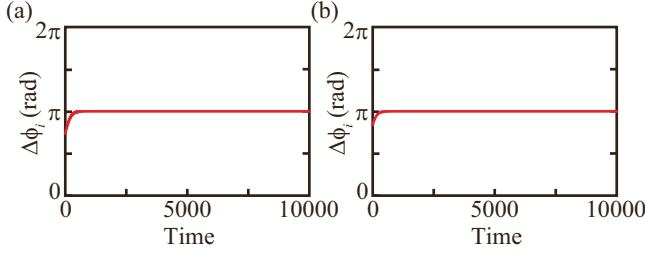


FIG. 9. Results of the numerical calculation for (a) a nonaveraged and (b) an averaged two-coupled system. Both systems show antiphase synchronization. For each calculation, the parameters are  $K = 0.001$  and  $\alpha = 1.0$ .

where we set

$$\begin{aligned} \Gamma_a(\theta_1) &= \Gamma(\pi + \theta_1) - \Gamma(\pi - \theta_1) \\ &= \begin{cases} -\frac{2}{\pi}\{(\pi + \theta_1) \sinh(\alpha\theta_1) + \theta_1 \sinh[\alpha(\pi + \theta_1)]\} \\ \quad \quad \quad (-\pi \leq \theta_1 \leq 0) \\ -\frac{2}{\pi}\{(\pi - \theta_1) \sinh(\alpha\theta_1) + \theta_1 \sinh[\alpha(\pi - \theta_1)]\} \\ \quad \quad \quad (0 \leq \theta_1 \leq \pi) \end{cases}. \end{aligned} \quad (30)$$

Equations (29) and (30) can be rewritten as

$$\frac{d\theta_1}{dt} \simeq K[\Gamma_a(0) + \Gamma'_a(0)\theta_1] = -\frac{2K}{\pi}[\pi\alpha + \sinh(\alpha\pi)]\theta_1. \quad (31)$$

Thus, we can see the antiphase synchronization is stable, which corresponds to Fig. 8(b). It should be noted that  $\Gamma(x)$  is not differentiable at  $x = \pi$  as can be seen in Eq. (22), but that  $\Gamma_a(\theta_1)$  is differentiable at  $\theta_1 = 0$  considering  $\Gamma(x)$  is antisymmetric around  $x = \pi$ .

In the numerical calculation, antiphase synchronization appeared stably for both nonaveraged and averaged models as shown in Fig. 9, which corresponds well to the results obtained by the linear stability analysis.

### B. Three-coupled system

In the nonaveraged coupling model, there is no fixed point that corresponds to the three-phase mode. In the averaged coupling model, generally,

$$\frac{d\psi_1}{dt} = K[\Gamma(\psi_1 - \psi_2) + \Gamma(\psi_1) - \Gamma(-\psi_1) - \Gamma(-\psi_2)], \quad (32)$$

$$\frac{d\psi_2}{dt} = K[\Gamma(\psi_2 - \psi_1) + \Gamma(\psi_2) - \Gamma(-\psi_1) - \Gamma(-\psi_2)]. \quad (33)$$

In Eqs. (32) and (33),  $\psi_1 = 4\pi/3$ ,  $\psi_2 = 2\pi/3$  and  $\psi_1 = 2\pi/3$ ,  $\psi_2 = 4\pi/3$  are the fixed points that correspond to the three-phase mode, and the equation to be considered is

$$\begin{aligned} \frac{d}{dt} \begin{pmatrix} \theta_1 \\ \theta_2 \end{pmatrix} \\ = K \begin{pmatrix} 2\Gamma'(\frac{2}{3}\pi) + \Gamma'(\frac{4}{3}\pi) & -\Gamma'(\frac{2}{3}\pi) + \Gamma'(\frac{4}{3}\pi) \\ \Gamma'(\frac{2}{3}\pi) - \Gamma'(\frac{4}{3}\pi) & \Gamma'(\frac{2}{3}\pi) + 2\Gamma'(\frac{4}{3}\pi) \end{pmatrix} \begin{pmatrix} \theta_1 \\ \theta_2 \end{pmatrix}. \end{aligned} \quad (34)$$

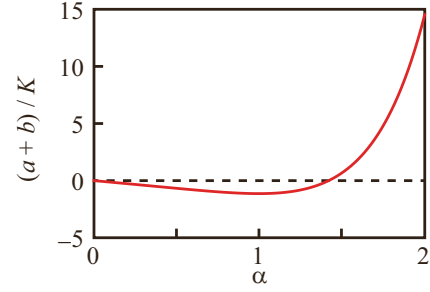


FIG. 10. Plot of  $(a+b)/K$  against  $\alpha$ . From the plot, it can be seen that bifurcation occurs at  $\alpha \simeq 1.5$ .

Now, we define the matrix  $A$  as

$$A = \begin{pmatrix} 2a+b & -a+b \\ a-b & a+2b \end{pmatrix}, \quad (35)$$

where  $a = K\Gamma'(2\pi/3)$  and  $b = K\Gamma'(4\pi/3)$ . Eigenvalues of  $A$  are calculated as

$$\lambda = \frac{3(a+b) \pm \sqrt{-3(a-b)^2}}{2}. \quad (36)$$

To discuss the stability of the fixed point, it is only necessary to consider the real part of the eigenvalues because the eigenvalues are complex conjugates. Since their real part is  $3(a+b)/2$ , the equation to be considered is

$$\begin{aligned} a+b &= K \left[ \Gamma' \left( \frac{2}{3}\pi \right) + \Gamma' \left( \frac{4}{3}\pi \right) \right] \\ &= 2\frac{K}{\pi} \left[ \sinh \left( \frac{1}{3}\pi\alpha \right) - \frac{2}{3}\pi\alpha \cosh \left( \frac{1}{3}\pi\alpha \right) \right. \\ &\quad \left. - \sinh \left( \frac{2}{3}\pi\alpha \right) + \frac{1}{3}\pi\alpha \cosh \left( \frac{2}{3}\pi\alpha \right) \right]. \end{aligned} \quad (37)$$

The plot of the real part of the eigenvalues of the system is shown in Fig. 10. From Eq. (37), we can calculate that a bifurcation occurs at  $\alpha = \alpha_c \simeq 1.419$ . If  $0 < \alpha < \alpha_c$ , the three-phase mode is stable.

From the numerical calculation, a quasistable three-phase mode, in which each phase difference was close to  $2\pi/3$  but was vibrating, so not exactly equal to  $2\pi/3$ , was observed when  $\alpha = 1.0$  in the nonaveraged model, as in Figs. 11(a) and 11(b). With the averaged model, the three-phase mode arose stably, when  $\alpha = 1.0$  as shown in Figs. 11(c) and 11(d), whereas, when  $\alpha = 2.0$ , the three-phase mode became unstable and a slow modulation of the phase difference around  $2\pi/3$  was observed in both the nonaveraged model [Fig. 11(e)] and the averaged model [Fig. 11(f)].

### C. Four-coupled system

In the numerical calculation, the behavior of the nonaveraged coupled system can vary with the parameter values of  $K$  and  $\alpha$  as shown in Fig. 12. We investigated the tendency to cluster with changing  $K$  and  $\alpha$ . In each condition, ten calculations were performed. To distinguish the state of the system, we defined three states and thresholds to classify the states as follows:

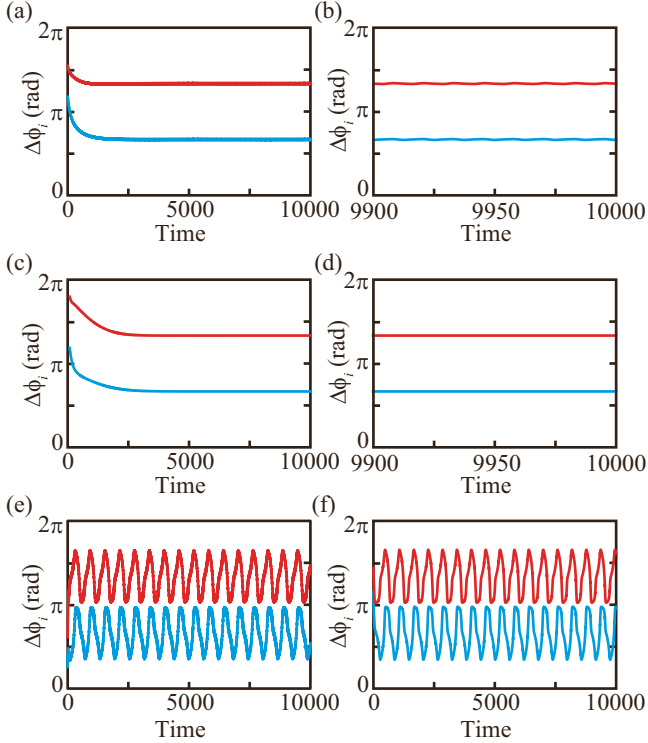


FIG. 11. Results of the numerical calculation for a three-coupled system. (a), (b) A nonaveraged system with  $\alpha = 1.0$ . (c), (d) An averaged three-coupled system with  $\alpha = 1.0$ . (b) and (d) are expanded figures of (a) and (c), respectively. (e) A nonaveraged three-coupled system with  $\alpha = 2.0$  and (f) an averaged three-coupled system with  $\alpha = 2.0$ . The averaged system shows a three-phase mode when  $\alpha = 1.0$ , whereas the nonaveraged system shows a quasistable three-phase mode with small fluctuation when  $\alpha = 1.0$ . Both averaged and nonaveraged systems show an unstable three-phase mode with a slow modulation of the phase difference, when  $\alpha = 2.0$ . For each calculation, we set  $K = 0.001$ .

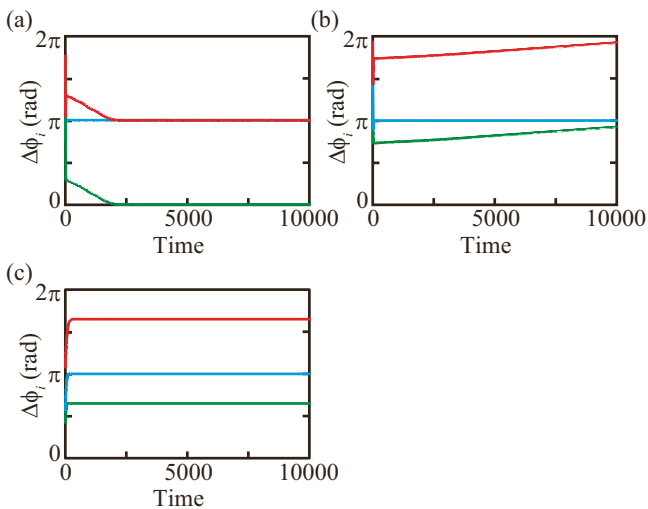


FIG. 12. Results of numerical calculation for a four-coupled system. The parameters are (a)  $\alpha = 1.5$ ,  $K = 0.03$ , (b)  $\alpha = 1.5$ ,  $K = 0.01$ , and (c)  $\alpha = 0.5$ ,  $K = 0.01$ .

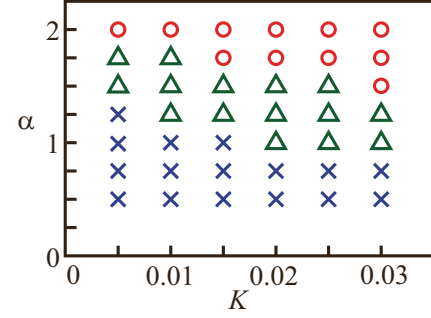


FIG. 13. Diagram obtained by the numerical calculation for a four-coupled system with various parameters. The red circle, blue cross, and green triangle represent the clustering state, nonclustering state, and ambiguous state, respectively. With higher  $K$  and  $\alpha$ , the system tends to show a clustering state.

1. Two-cluster state: In this state, the phase difference between two of four oscillators and that between the other two oscillators are both smaller than  $2\pi \times 10^{-3}$  in  $t = 8000$  to  $10\,000$ . The phase difference between the two pairs of oscillators are around  $\pi$ . For example, in Fig. 12(a), two pairs of two oscillators are at the same phase and the phase difference of the two pairs is  $\pi$ .

2. 2-2 mode: In this state, the time changes of the phase differences for all oscillators for every time step are always  $< 2\pi \times 10^{-3}$  in  $t = 8000$  to  $10\,000$ . For example, in Fig. 12(c), two pairs of oscillators have phase differences fixed at  $\pi$ , and the phase difference of these pairs is fixed at a constant value.

3. Ambiguous state: This state describes any state other than those listed above.

The calculation results are shown in Fig. 13. The 2-2 cluster state appeared more frequently for larger  $K$  or  $\alpha$ .

We also performed a numerical calculation for a four-coupled system with the averaged model. In this calculation, we observed the 2-2 mode but never observed any clustering state under any conditions we tried.

## V. EXPERIMENT: MEASUREMENT OF THE PHASE-RESPONSE CURVE

To obtain the phase response of a density oscillator, we performed the following experiment: Fresh water in the outer vessel of a single density oscillator and a pipette were connected with a rubber tube. The water level was measured with a laser displacement meter (LT9010M, Keyence). By adding or removing a fixed amount of fresh water with the pipette at an arbitrary phase, the system was perturbed as shown in Fig. 14. Because water was added or removed alternately, the cumulative effect of addition and removal of water was negligible. Based on these results, the phase response was obtained by plotting the phase shift versus the phase at which the perturbation was added. The ratio of pressure added through one perturbation,  $P_{\text{pert}}$ , to the amplitude of the pressure difference,  $\Delta P_{\text{amp}} \equiv \max(\Delta P) - \min(\Delta P)$ , is  $P_{\text{pert}}/\Delta P_{\text{amp}} \approx 0.17$ .

The phase response of a density oscillator has already been obtained experimentally by González *et al.* by using a pulselike perturbation [20]. In our study, the perturbation is a single

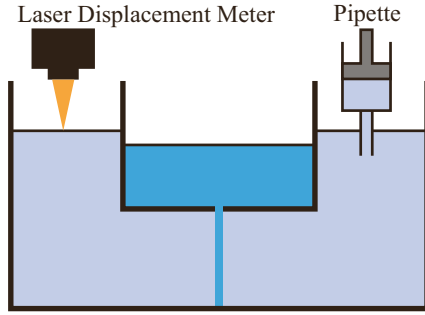


FIG. 14. Schematic illustration of the side view of the experimental system to measure the phase response.

addition or single removal of water, which is easy to relate to the change in water level resulting from other oscillators' evolution in a coupling system.

To obtain the phase shift, we constructed a linear fit of the phase evolution both before and after the perturbation. As a phase before the perturbation, we used the data in three periods just before the perturbation. As a phase after the perturbation, we used the data in the three periods that occur two periods after the perturbation, as shown in Fig. 15, because the transient period of a density oscillator after a perturbation was sufficiently short and we consider the oscillator to have returned to the limit cycle during the following two or fewer cycles. Then the phase was determined with the same procedure as in the previous part, and a fitting was performed with a fixed slope, i.e., using the same phase velocity  $\omega$  for both before and after the perturbation. Therefore, we fitted the experimental data with two linear equations and determined  $\phi_B$  and  $\phi_A$  before and after the perturbation:

$$\begin{aligned} \phi_B(t) &= \omega t + \phi_0 \quad (\text{before perturbation}), \\ \phi_A(t) &= \omega t + \phi_1 \quad (\text{after perturbation}). \end{aligned} \quad (38)$$

Then, the phase shift  $\Delta\phi$  is calculated using

$$\Delta\phi = \phi_1 - \phi_0, \quad (39)$$

and phase response  $Z$  is

$$Z = \begin{cases} \Delta\phi, & (\text{If water is added}) \\ -\Delta\phi, & (\text{If water is removed}) \end{cases} \quad (40)$$

The phase at which the perturbation is added,  $\phi$ , is calculated using  $(t_p - t_0)\omega$ , where  $t_p$  and  $t_0$  are the time at which the perturbation is added and that which corresponds

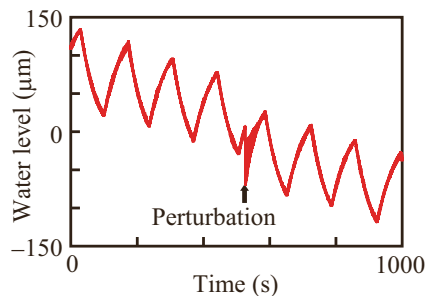


FIG. 15. Experimental results for the phase-response curve.

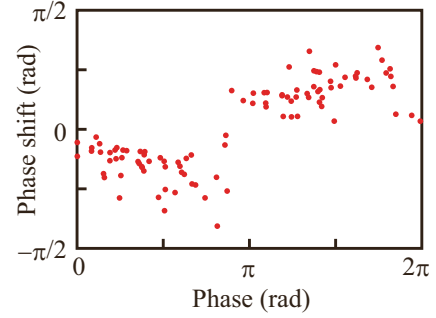


FIG. 16. Phase response calculated from the experimental results.

to the phase equal to zero in the period just before the perturbation, respectively.

Figure 16 shows the relationship between  $Z$  and  $\phi$ , namely, the phase-response curve that was obtained experimentally. It can be seen that the tendency of the phase-response curve obtained in experiments is similar to the one obtained theoretically shown in Fig. 7.

## VI. CONCLUSION

In this article, we suggested a method to obtain the phase response of a density oscillator. The model derived is considered to reflect the features of the experimental system in the sense that we can obtain similar synchronization behaviors in the model and the experiment.

This method is so general that we can apply it to other oscillator systems. If the relation between an essential physical value and the phase is known, we can determine the phase response mathematically from the relation. In the case of a density oscillator, we assume that the oscillation is driven by the pressure difference around a bore, and we derive the relation between the phase and the pressure difference. Even if the relation between an essential physical value and the phase is unclear, it might be possible to obtain the relation phenomenologically using the experimental observation.

In addition, Okuda pointed out a relation between the clustering mode and the Fourier components of the coupling function [8]. Therefore, if we can apply the results to the phase response derived by our method, it might be possible to predict the clustering mode by only considering the phase response of a single oscillator based on physics as we did in this article. Today we have only one example of an application of this method, so we need to apply it to other systems to develop the method further.

## ACKNOWLEDGMENTS

This work was supported in part by Grants-in-aid for Scientific Research (C) to H.K. (Grant No. 26520205), and for Scientific Research on Innovative Areas "Fluctuation & Structure" to T.S. and H.K. (Grant No. 25103008), and the Core-to-Core Program "Nonequilibrium dynamics of soft matter and information" to H.K. from MEXT, Japan.



- [1] Y. Kuramoto, *Chemical Oscillations, Waves, and Turbulence* (Springer, New York, 1986).
- [2] H. Kitahata, J. Taguchi, M. Nagayama, T. Sakurai, Y. Ikura, A. Osa, Y. Sumino, M. Tanaka, E. Yokoyama, and H. Miike, *J. Phys. Chem. A* **113**, 8164 (2009).
- [3] K. Miyakawa and K. Yamada, *Physica D* **151**, 217 (2001).
- [4] W. Wang, I. Z. Kiss, and J. L. Hudson, *Chaos* **10**, 248 (1999).
- [5] R. de Haan and H. Sachs, *Curr. Top. Dev. Biol.* **7**, 193 (1972).
- [6] I. Aihara, *Phys. Rev. E* **80**, 011918 (2009).
- [7] D. Hansel, G. Mato, and C. Meunier, *Phys. Rev. E* **48**, 3470 (1993).
- [8] K. Okuda, *Physica D* **63**, 424 (1993).
- [9] M. R. Tinsley, S. Nkomo, and K. Showalter, *Nat. Phys.* **8**, 662 (2012).
- [10] H. Kori and Y. Kuramoto, *Phys. Rev. E* **63**, 046214 (2001).
- [11] J. Miyazaki and S. Kinoshita, *Phys. Rev. Lett.* **96**, 194101 (2006).
- [12] H. Kori, Y. Kuramoto, S. Jain, I. Z. Kiss, and J. L. Hudson, *Phys. Rev. E* **89**, 062906 (2014).
- [13] S. Martin, *Geophys. Fluid Dyn.* **1**, 143 (1970).
- [14] S. Nakata, T. Miyata, N. Ojima, and K. Yoshikawa, *Physica D* **115**, 313 (1998).
- [15] K. Yoshikawa, N. Oyama, M. Shoji, and S. Nakata, *Am. J. Phys.* **59**, 137 (1991).
- [16] M. Okamura and K. Yoshikawa, *Phys. Rev. E* **61**, 2445 (2000).
- [17] O. Steinbock, A. Lange, and I. Rehberg, *Phys. Rev. Lett.* **81**, 798 (1998).
- [18] K. Aoki, *Physica D* **147**, 187 (2000).
- [19] T. Kano and S. Kinoshita, *Phys. Rev. E* **80**, 046217 (2009).
- [20] H. González, H. Arce, and M. R. Guevara, *Phys. Rev. E* **78**, 036217 (2008).
- [21] A. T. Winfree, *J. Theor. Biol.* **16**, 15 (1967).